Starch - Stärke

WILEY-VCH

Starch

RESEARCH ARTICLE OPEN ACCESS

Extraction and Comprehensive Characterization of Starch From Ryegrass (*Lolium multiflorum* L.) Seeds as a Non-Conventional Source

Thaís Silveira Pimenta[1] | Geycson Figueiredo Dias[1] | Hugo José Martins Carvalho[1,2] | Nathalia de Andrade Neves[1] | Sérgio Michielon de Souza[3] | Carlos Wanderlei Piler de Carvalho[4] | Elizabeth Harumi Nabeshima[5] | Izabela Dutra Alvim[5] | Maria Teresa Pedrosa Silva Clerici[2] | Mária Herminia Ferrari Felisberto[6] | Marcio Schmiele[1,2]

[1]Institute of Science and Technology, Federal University of the Jequitinhonha and Mucuri Valleys (UFVJM), Campus JK, Diamantina, Minas Gerais, Brazil | [2]Department of Food Science and Nutrition, University of Campinas (UNICAMP), Campinas, São Paulo, Brazil | [3]Department of Materials Physics, Federal University of Amazonas (UFAM), Manaus, Amazonas, Brazil | [4]Embrapa Food Technology, Brazilian Agricultural Research Corporation (EMBRAPA), Rio de Janeiro, Rio de Janeiro, Brazil | [5]Institute of Food Technology (ITAL), Campinas, São Paulo, Brazil | [6]Department of Food Technology, Federal University of Viçosa (UFV), Viçosa, Minas Gerais, Brazil

Correspondence: Marcio Schmiele (marcio.sc@ict.ufvjm.edu.br)

Received: 20 March 2025 | **Revised:** 4 September 2025 | **Accepted:** 15 December 2025

Keywords: extraction yield | gelatinization temperature | granule size | unconventional starch

ABSTRACT

Our research group focused on natural, but unexploited starches, specifically ryegrass seed starch, which was obtained using aqueous (AE) and reducing (RE) extraction. The physical-chemical, structural, morphological, rheological, and nutritional properties were evaluated. RE starch showed a higher yield (37.81%) compared to AE (31.55%) and exhibited higher luminosity and transmittance, making it the clearest sample. AE starch exhibited a mean particle size (D_{50}) of 6.95 ± 0.08 μm, whereas RE starch showed a mean particle size (D_{50}) of 7.54 ± 0.07 μm. Both starches presented small variations among samples and an irregular trimodal particle size distribution. The apparent amylose content of RE starch (17.25%) was higher than AE. RE starch exhibited greater solubility with increasing temperature, reaching a maximum of 7.27 g of gel/g of sample. The highest swelling power (2.56%) was observed in RE starch. RE extraction also resulted in a higher paste temperature (95°C) and greater retrogradation tendency (2954 mPa.s). The highest syneresis occurred at 48 h, with AE and RE showing 24.20% and 27.58%, respectively. RE starch increased both rapidly and total starch digestibility, while slowly digestible and resistant starch fractions, as well as the glycemic index, remained unaffected.

1 | Introduction

Ryegrass seeds (*Lolium multiflorum* L.), a *Poaceae* species native to southern Europe, northern Africa, and western Asia, are characterized by deep green coloration, prolific tillering, and a vegetative height ranging from 0.75 to 1.2 m. This winter plant features straight cylindrical culms, reddish nodes, hairless sheaths, and smooth, shiny leaves. Its rustic nature, ease of cultivation, and pest resistance enhance its agricultural utility [1, 2].

Ryegrass is a high-yield crop that remains underutilized for human consumption but holds significant potential for innovation and expanding the global food supply. Its morphological, agronomic, and nutritional attributes are appealing, particularly its strong resistance to pests and adaptability to a variety of

soil types. It also shows favorable adaptation to regions located partially or entirely below the Tropic of Capricorn or above the Tropic of Cancer [3]. Ryegrass seeds are primarily used as forage for animal feed and as a soil cover in conservation systems, including no-till farming, due to their adaptability to low to medium-fertility soils, low seed cost, rapid establishment, cold tolerance, and disease resistance [4].

The ryegrass seed is classified as a hulled caryopsis with smaller morphometric dimensions compared to rice grains. It has a rich composition of structural components, including non-digestible oligo and polysaccharides in the cell walls, as well as reserve components such as proteins, lipids, and digestible carbohydrates. Starch and sugars are key constituents, supplying carbon for energy and supporting seed maintenance during storage and germination [2].

Ryegrass has emerged as a promising alternative starch source, owing to its high content of digestible carbohydrates (63.69 ± 0.43) [2]. As an unconventional starch source, it differs from traditional ones (such as corn, potato, and rice) in cultivation patterns, extraction methods, and applications, as it is typically grown for other purposes and on a smaller scale [5]. The valorization of such alternative sources is driven by global population growth, the demand for more sustainable agricultural practices, the utilization of by-products, the cultural and social relevance of the starch source, its technological advantages over common starches, and the promotion of regional crops. Additionally, certain technical advantages in modification and application have been reported when compared to conventional starches [6].

Nevertheless, its starch characteristics remain largely unexplored, with no documented protocols for extraction, isolation, or purification, nor data on its morphological, structural, rheological, or nutritional properties. Starch granules exhibit considerable morphological variability and a broad size distribution. They are commonly classified into A-type granules, with diameters greater than 15 μm; B-type granules, ranging from 5 to 15 μm; and C-type granules, with diameters smaller than 5 μm [7]. On C-type granules, there's another classification of native starches known as nano-starch, with its first appearance in Goering and associates' work [8], originating from cow cockle seeds with a starch granule diameter ranging from 0.5 to 1.6 μm. The use of native nano-starch offers opportunities for novel applications and the utilization of underexplored grasses. Native nano-starch can partially or fully replace nano-starch produced by chemical or physical methods, thereby supporting more sustainable production routes, reducing processing costs, and mitigating environmental impacts [9].

The extraction of native starch varies from minimal modification methods, such as water-based processes, to reductive approaches that alter starch characteristics. This study aimed to investigate ryegrass seeds as a novel source of starch and to evaluate their potential as an unconventional starch. The extraction process was assessed, and the physicochemical, technological, morphological, structural, and rheological properties of the extracted starch were comprehensively characterized, targeting not only food applications but also broader industrial-scale applications.

2 | Materials and Methods

2.1 | Raw Material

Ryegrass seeds (Uruguayan Winter Star 3 cultivar) were purchased in São Lourenço do Sul, Brazil, and the study was registered in the Brazilian SisGen system (registration no. ADE0BDA). All chemical reagents were of analytical grade, meeting the required methodological purity standards.

2.2 | Physical Characterization of Ryegrass Seeds

Ryegrass seeds with husked caryopsis were characterized (n = 3) for morphometric measurements, thousand-grain weight, and test weight, as described by Lima et al. [2]. The length and thickness of 50 grains were measured with a 150 mm analog caliper (Western, Suzhou, China). Thousand-grain weight (g) was calculated by weighing 200 grains and multiplying by five. Test weight ($kg \cdot hL^{-1}$) was determined by measuring the grain weight in a 250 mL volumetric container, repeated four times, using an AUY 220 analytical balance (Shimadzu, Piracicaba, Brazil).

2.3 | Proximate Composition of Ryegrass Seeds

Ryegrass seeds were ground to a particle size smaller than 150 μm using a TE-350 ball mill (Tecnal, Piracicaba, Brazil) and evaluated according to moisture, protein (N = 6.25), lipid, ash and starch contents following the methods 44-15.02, 46-13.01, 30-25.01, 08-01.01, and 76-13.01 from American Association of Cereal Chemists International (AACCI) [10], respectively. Total dietary fiber content was calculated by difference. All analyses were performed in triplicate, and the results were expressed as $g \cdot 100\ g^{-1}$.

2.4 | Starch Isolation

The ryegrass seeds were milled into flour using a multigrain disk grinder (Malta, Caxias do Sul, Brazil) to achieve a particle size < 350 μm. Hulled caryopses were used in the wet milling process, as this reflects their typical usage. Dehulling was not performed due to the unavailability of appropriate equipment and the impracticality of manual removal, given the very small size of the ryegrass seeds.

Starch was extracted using aqueous extraction (AE) and reducing extraction (RE), following methodologies from El Halal et al. [11], with some modifications. AE was chosen because it is the simplest, cheapest, and most environmentally friendly method. On the other hand, sodium bisulfite was used as a reducing agent (0.2% active SO_2) in the RE to disrupt protein bonds, facilitate starch granule release, and act as an antimicrobial and bleaching agent.

Ryegrass seed flour (120 g) was mixed with 0.48 L of extraction solution using a PMX 700 mixer (Philco, Curitiba, Brazil) at maximum speed for 2.5 min. After the resting at room temperature for 18 h, the mixture underwent additional mixing (3 min), filtration (88 μm sieve), decantation (17 h, 1 L cylinder), siphoning (gravity,

5 mm hose), centrifugation (3200 × *g*, 10 min, 20°C, Sorvall ST 8 centrifuge), and purification by resuspension and centrifugation. The starch was then resuspended in analytical-grade ethanol, recovered by filtration (Unifil filter paper, 9 cm, 80 g.m^{-2}), dried (40°C, 12 h, TE-394/1 oven), ground (< 150 µm, TE-350 ball mill), and stored in low-density polyethylene. Extractions were performed in triplicate, with yield calculated on a dry basis using Equation (1).

$$\text{Yield}(\%) = \frac{weight\ of\ ryegrass\ starch(g)}{weight\ of\ reygrass\ flour(g)} \cdot 100 \quad (1)$$

2.5 | Physicochemical Characterization of Ryegrass Seeds Starch

2.5.1 | Proximate Composition

The proximate composition of ryegrass seeds starch was analyzed in triplicate according to AACCI methods: moisture (44-15.02), protein (46-13.01; $N = 6.25$), ash (08-01.01), and lipid (30-25.01) contents [10]. Total carbohydrates were calculated by difference.

2.5.2 | Apparent Amylose

The apparent amylose content was determined via a colorimetric method with an iodine/potassium iodide solution, as described by Schmiele et al. [12] and calculated by Equation (2).

$$\text{Apparent amylose content}(\%) = (A^*K^*100)/M \quad (2)$$

where A = absorbance of the sample; $K = 2.377691547$ (derived from maize amylose/amylopectin standards); M = weight of the sample.

2.5.3 | Damaged Starch

The damaged starch content was determined in triplicate using the method 76-33.01 from AACCI, and the results were expressed as a percentage [10].

2.5.4 | Elementary Minerals

The mineral profile was analyzed from the ash derived from starch samples obtained through proximate composition analysis using energy-dispersive x-ray fluorescence spectrometry (EDX-720, Shimadzu, Kyoto, Japan) on air-dried fine soil. The ash was placed in a 32 mm diameter and 23 mm height polyethylene holder sealed with a 6 µm Mylar film under vacuum. The spectrometer operated at 15 keV for elements Na–Sc, 50 keV for Ti–U, with a 10 mm collimator, a 200 s integration time, and a Si(Li) detector cooled by liquid nitrogen.

2.5.5 | Instrumental Color

The instrumental color determination was conducted using a CM5 spectrophotometer (Konica Minolta, Tokyo, Japan), employing the CIELab color system with a D65 illuminant, a 10° observer angle, and the RSIN—reflectance specular included calibration mode [12]. The L^*, a^*, b^* and the whiteness index were evaluated in triplicate.

2.6 | Morphological Characterization of Ryegrass Seed Starch

The morphology of the granules was analyzed by scanning electron microscopy (SEM) using a TM3000 microscope (Hitachi, Tokyo, Japan). Samples were mounted on carbon foil and coated with gold. Images were captured at an acceleration voltage of 15 kV and a beam current of 33.9 µA, with magnifications of 1500× and 5000× [12].

The particle size distribution of the samples was determined by laser diffraction (dynamic light scattering—DLS) (HORIBA LA-950 V2, Irvine, California). The samples were dissolved in absolute ethanol and introduced into the equipment's analysis module until the appropriate transmittance levels were reached. The parameters used as results were D_{10}, D_{50} (median or mean diameter), and D_{90} [13]. Analyses were performed in six replicates. The polydispersity index (PDI) was calculated using Equation (3).

$$\text{PDI} = (D_{90} - D_{10})/D_{50} \quad (3)$$

2.7 | Structural Characterization of Ryegrass Seeds Starch

2.7.1 | X-Ray Diffraction (XRD)

XRD analysis was conducted using an XRD-6000 (Shimadzu, Tokyo, Japan) with a rotating Cu anode at 40 kV and 30 mA. Diffraction angles ranged from 5° to 70° (2θ) with a 0.02° step size and a scanning speed of 2° min^{-1}. Crystallinity (x_c) was determined as the ratio of the "Rietveld Refinement" curve area to a 13-term Chebyshev polynomial.

2.7.2 | Fourier-Transform Infrared Spectroscopy (FTIR)

The samples were analyzed using a Cary 630 FTIR (Agilent Technologies, California, United States). The absorbance range was set between 4000 and 400 cm^{-1}, with a resolution of 4 cm^{-1} and a total of 8 scans performed [12].

2.7.3 | Differential Scanning Calorimetry (DSC)

The thermal properties of the samples were analyzed using a DSC-60 (Shimadzu, Kyoto, Japan) as described by Schmiele et al. [12]. A 3 mg (d.w.) sample and 7 µL of deionized water were sealed in aluminum capsules, equilibrated at room temperature for 1 h, and measured against an empty capsule reference. Scanning was performed from 30°C to 95°C at 5°C·min^{-1}. Thermograms provided values for initial temperature (T_{on}-°C), peak temperature (T_{peak}-°C), final temperature (T_{end}-°C), and gelatinization enthalpy (ΔH-J·g^{-1}), in triplicate.

2.8 | Rheological Characterization of Ryegrass Seed Starch

2.8.1 | Swelling Power and Solubility

A 0.5 g sample (d.w.) was weighed in triplicate into 15 mL centrifuge tubes, followed by adding 10 mL distilled water. The tubes were capped and incubated in a TE-052 water bath (Tecnal, Piracicaba, Brazil) at 25°C, 50°C, 60°C, 70°C, and 80°C with intermittent manual agitation, as described by Schmiele et al. [12]. After 30 min, centrifugation at 2200 × *g* for 10 min in a 206BL centrifuge (Fanem, Guarulhos, Brazil) was performed to separate phases. The supernatant was dried in a TE-394/1 forced-air oven (Tecnal, Piracicaba, Brazil) to constant weight for soluble fraction quantification (Equation 4). The swollen starch granules were weighed to determine swelling power (Equation 5).

$$\text{Solubility } (\%) = \frac{\text{Leached starch weight (g)}}{\text{Initial starch weight (g)}} \times 100 \quad (4)$$

$$\text{Swelling power } \left(\text{g} \cdot \text{g}^{-1}\right) = \frac{\text{Final weight of the swollen starch (g)}}{\text{Initial starch weight (g)} - \text{Leached starch weight (g)}} \quad (5)$$

2.8.2 | Pasting Properties

The pasting properties were analyzed using method 76-21.01 from AACCI [10], with an RVA-4500 Rapid Visco-Analyzer (Perten, Warriewood, Australia). A sample (2.5 g, 14% moisture) was prepared with 25 g of water, and the Standard 1 profile was applied, evaluating the pasting temperature (T_p), peak viscosity (V_p), peak time, breakdown viscosity (BV), final viscosity (V_f), and setback viscosity. Analyses were performed in triplicate, with results reported as °C (T_p), min (peak time), and mPa·s (other parameters).

2.8.3 | Gel Strength

The gel strength of starch samples was measured as described by Schmiele et al. [12]. Starch gels (8% solids, w/w) were prepared using an RVA-4500, transferred to 50 mL cylindrical containers, and stored at 7°C for 24 h. Before analysis, the gels were equilibrated at room temperature for 2 h. Gel strength (N) was assessed using a TA-XT2i texture analyzer (Stable Micro Systems, Haslemere, England) equipped with a 25 kg load cell. The conditions included pre-test, test, and post-test speeds of 5.0, 1.0, and 1.0 mm·s^{-1}, a penetration distance of 10.0 mm, a detection limit of 0.05 N, and a Derlin P/10 cylindrical probe. Nine replicates were performed.

2.8.4 | Paste Clarity

The paste's clarity was assessed by dispersing 0.1 g of starch (d.w.) in 10 mL of distilled water. The suspension was heated in a boiling water bath for 30 min and cooled to room temperature, and its transmittance percentage was measured at 650 nm using a spectrophotometer, with distilled water as the blank [14].

2.8.5 | Syneresis During Freezing-Thawing

The stability of freezing-thawing was evaluated using a modified method based on Wu et al. [15]. Starch-water solutions (3.0%, w/w) were stirred at 94°C for 30 min. After cooling to 25°C, the starch pastes were placed in 50 mL Falcon tubes and stored at −20°C for 48 h. Thawing was conducted in a water bath at 30°C for 2 h. This cycle was repeated seven times (336 h). Gels were centrifuged at 3500 × *g* for 15 min, and the supernatants were completely removed. The syneresis percentage (SP) was determined using Equation (6).

$$\text{Syneresis percentage}(\%) = (w_1 - w_2)/(w_1 - w_0) \quad (6)$$

where w_0 = weight of the centrifuge tube, w_1 = weight of the centrifuge tube and sample before the freezing-thawing process, and w_2 = weight of the centrifuge tube and sample after the freezing-thawing cycle.

2.9 | Starch Digestibility and Glycemic Index (GI)

The digestibility of ryegrass seed starches was evaluated using the enzymatic kit K-DSTRS 07/2023 (Megazyme International Ltd., Bray, Ireland). Native starch (250 mg) was incubated with pancreatic α-amylase (8 KU) and amyloglucosidase (1.7 KU) under controlled conditions in a Dubnoff 304/D water bath (Nova Ética, Piracicaba, Brazil) at 37°C with 150 rpm agitation. Enzymatic activity was halted at specific intervals by mixing 1000 µL aliquots with 20 mM acetic acid. Glucose released during hydrolysis was measured using the GOD-POD reagent. Starches were classified based on hydrolysis rates as rapidly digestible (RDS, hydrolyzed within 20 min), slowly digestible (SDS, hydrolyzed within 120 min), total digestible (TDS, hydrolyzed within 240 min), and resistant starch (RS, not hydrolyzed within 240 min). The in vitro GI was calculated from the hydrolysis rate at 90 min following the method of Gõni et al. [16].

2.10 | Statistical Analysis

The results obtained were evaluated using the Student's *t* test, with a significance level of 5%.

3 | Results and Discussion

3.1 | Physical Characterization of Ryegrass Seeds

The morphometric characteristics of ryegrass seeds reveal an average length of 5.01 ± 0.78 mm and a thickness of 1.36 ± 0.32 mm, which are smaller than those of long-grain rice (length ~6 mm, thickness ~1.85 mm). The thousand kernel weight was measured at 3.70 ± 0.07 g, while the hectoliter weight was recorded as 49.93 ± 0.12 kg·hL^{-1}. Variations in hectoliter weight are influenced by moisture content, and an inverse relationship between protein content and hectoliter weight has

been established in cereal science. Although comparative data for other ryegrass seed varieties are unavailable, these metrics were determined to facilitate comparisons within the species. For context, hectoliter weight values typically range between 78 and 86 kg·L^{-1} for yellow maize [17] and 55 and 60 kg·L^{-1} for paddy rice [18]. These findings may contribute to the development of the ryegrass seed production chain.

3.2 | Proximate Composition of Ryegrass Seeds

The ryegrass seeds (hulled caryopsis) were determined to have an average moisture content of 10.16 ± 0.19 g·100 g^{-1}. The ash content was quantified at 5.08 ± 0.09 g·100 g^{-1}, lipids at 0.31 ± 0.01 g·100 g^{-1}, protein at 12.86 ± 0.44 g·100 g^{-1}, dietary fibers at 7.66 ± 0.43 g·100 g^{-1}, and starch content at 63.93 ± 4.36 g·100 g^{-1}. These findings highlight the potential of ryegrass seeds as an unconventional source of starch. Lima et al. [2] evaluated whole ryegrass seeds of the cultivar RG-LE1963 and reported starch and dietary fiber contents of 71.16 and 7.79 g·100 g^{-1}, respectively (d.w). Variations in compositional data may be attributed to differences in variety, cultivation conditions, climate, soil type, harvesting practices, storage, and other factors that influence the grain's characteristics.

3.3 | Ryegrass Seeds Starch Extraction Yield

A significant difference ($p = 0.038$) in starch extraction yield was observed between the two methods evaluated for ryegrass seeds. The AE method produced a yield of 31.55 ± 2.55%, whereas the RE method achieved a higher yield of 37.81 ± 1.41%. When adjusted for the starch content in ryegrass seeds, the yields increased to 49.35% and 59.14% for the AE and RE methods, respectively. Extraction yield represents a critical parameter in industrial applications, as it directly impacts processing costs, effluent generation, and waste management requirements [19]. In the present study, the yield additionally served as an indicator of technological quality and starch purity, with lower contents of proteins, lipids, ash, and dietary fiber being desirable.

Given the novel focus of this research on ryegrass seed starch, no comparable data were found in the literature regarding extraction yields or method efficiency. However, as the extraction process utilized ryegrass seed flour containing the husk, due to processing limitations and the lack of equipment for efficient husk removal, the yield was considered low compared to other starch sources. For example, Silva et al. [20] reported AE yields of 47% for red rice, 44% for white rice, and 36% for black rice. Another study has documented a yield of 62% for maize starch using the reducing method [21].

The highest yield in the present study was obtained with the RE extraction method, which was attributed to the disruption of disulfide bonds within the protein matrix [22]. This effect was facilitated by the action of sulfite as a reducing agent, enhancing the leaching of starch granules and promoting their separation, thereby increasing the overall extraction yield.

3.4 | Instrumental Color of Ryegrass Seed Starch

The starches obtained presented a whiteness index of 85 for the aqueous sample (AE), and 90 for the reducing sample (RE) (Table S1) and were classified as acceptable in terms of purity, as described by Costa et al. [22]. The higher luminosity (91.01) observed for RE starch can be attributed to the effect of the reducing agent employed, which likely inhibited enzymatic activity and facilitated the degradation of natural pigments, such as carotenoids and phenolic compounds (primarily flavonoids). Color is an important quality attribute, particularly in industrial and food applications, as it influences consumer acceptance, indicates the degree of purification, and reflects the presence of pigments or impurities originating from the raw material or processing conditions. Accordingly, color measurements provide valuable complementary information for starch quality. The results obtained corroborate the efficiency of the extraction methods and indicate effective preservation of the native starch color.

3.5 | Chemical Composition of Ryegrass Seed Starch

The extraction processes employed yielded starches with high protein content and low levels of ash and lipids (Table 1). The percentage of total carbohydrates reflects the content of digestible carbohydrates (starch) and non-digestible carbohydrates (dietary fiber). Both samples demonstrated values exceeding 88 g·100 g^{-1}, indicating the high purity of the starches obtained on a laboratory scale, irrespective of the extraction method employed (AE or RE). However, it should be noted that higher starch purity from ryegrass seeds may be achieved using industrial equipment with purification capabilities, highlighting a limitation of laboratory-scale processes.

The starches extracted from ryegrass seeds were found to exhibit apparent amylose contents comparable to those of conventional cereal and unconventional starches, which typically range from 20% to 30% [23]. The apparent amylose content of starch AE was determined to be 16.90%, whereas starch RE exhibited a value of 17.25% (Table 1), with no significant difference observed between the two samples ($p > 0.05$).

The physical structure of starch granules may be disrupted during the extraction process, leading to increased water absorption and greater susceptibility to enzymatic hydrolysis by amylolytic enzymes. Such damage is primarily attributed to the mechanical forces applied during milling. In this study, the reducing agent led to greater disruption of the protein matrix and increased leaching of RE starch granules (Table 1). This resulted in enhanced friction and shear forces between the granules and the rotating blades of the mixer during extraction, thereby producing a higher content of damaged starch and a greater extraction yield when compared to AE starch obtained via the aqueous method.

The ash content, which is directly associated with the mineral content, represents the inorganic residue remaining after the combustion of organic material. The AE starch was found to contain a higher phosphorus (P) content (150 mg·100 g^{-1}), whereas

TABLE 1 | Proximate composition, amylose content, damaged starch, and elemental minerals of ryegrass starches obtained by aqueous and reducing extractions.

Component	Aqueous extraction starch	Reducing extraction starch	*p* value
Moisture (g·100 g^{-1})	7.96 ± 0.37	6.45 ± 0.41	0.439
Proteins (g·100 g^{-1})[c]	2.70 ± 0.07	2.15 ± 0.03	< 0.001
Ashes (g·100 g^{-1})[c]	0.68 ± 0.03	0.77 ± 0.03	0.012
Lipids (g·100 g^{-1})[c]	0.06 ± 0.01	0.01 ± < 0.01	0.004
Total carbohydrates (g·100 g^{-1})[a,b]	88.60 ± 0.38	90.62 ± 0.41	0.468
Apparent amylose (%)	16.90 ± 0.77	17.25 ± 0.57	0.352
Damage starch (%)[c]	10.29 ± 0.10	11.12 ± 0.11	< 0.001
Elementary minerals			
Si (mg·100 g^{-1})[c]	147 ± 10	194 ± 10	0.022
P (mg·100 g^{-1})	150 ± 5	166 ± 7	0.522
Ca (mg·100 g^{-1})[c]	126 ± 4	122 ± 3	< 0.001
K (mg·100 g^{-1})[c]	115 ± 7	69 ± 6	< 0.001
S (mg·100 g^{-1})[c]	82 ± 5	152 ± 8	< 0.001
Fe (mg·100 g^{-1})[c]	37 ± 2	35 ± 2	0.005
Ag (mg·100 g^{-1})	18 ± 1	20 ± 2	0.184
Cu (mg·100 g^{-1})[c]	14 ± 1	13 ± 2	0.015

Data are the means ± standard deviation of three replicates.
[a]Value calculated by difference (100 − ∑moisture, protein, ashes, lipids).
[b]Standard deviation calculated by the propagation of error.
[c]A significant difference was observed between the samples ($p < 0.05$).

the RE starch exhibited greater silicon (Si) content (194 mg·100 g^{-1}). Silicon has been demonstrated to confer significant health and esthetic benefits. Studies have indicated that oral silicon supplementation may prevent skin aging and the weakening of hair and nails, thereby promoting overall health. Silicon is present in higher concentrations in certain foods, such as watercress (610.6 mg·100 g^{-1}), wheat bran (67.8 mg·100 g^{-1}), and green beans (43.9 mg·100 g^{-1}), among others [24]. In addition to silicon and phosphorus, other minerals, including calcium (Ca), potassium (K), sulfur (S), iron (Fe), copper (Cu), and silver (Ag), have also been identified in ryegrass seed starch (Table 1).

3.6 | SEM and Size Analysis of Ryegrass Seeds Starch

The shape and size of the starch granules were examined using SEM and DLS. The images and size distribution profiles obtained for starches extracted by AE and RE from ryegrass seeds (Figure 1 and Table 1) allowed the granules to be classified into three size groups. For RE starch, 20% of the granules exhibited diameters smaller than 5 μm (Type C), 40% ranged between 5 and 15 μm (Type B), and 40% had diameters greater than 15 μm (Type A). In contrast, AE starch consisted of 30% Type C granules, 40% Type B granules, and 30% Type A granules. This size distribution indicates that ryegrass seed starch can be classified as a trimodal starch. In terms of morphology, the starch granules exhibited oval, polyhedral, and irregular shapes.

The average granule size of the RE starch was determined to be 7.54 ± 0.07 μm (D_{50}), with a size range of 3.28 to 193.56 μm. In contrast, the AE starch exhibited an average granule size of 6.95 ± 0.08 μm (D_{50}), with values ranging from 2.79 to 104.32 μm.

The size of the starch granules was influenced by the extraction method, since the mechanical force, combined with the extraction method, can cause granule shearing, leading to alterations in size distribution and granule integrity as described by Rashwan et al. [25]. Smaller granules demonstrated a tendency to sediment more slowly [26]. Consequently, the presence of very small granules in ryegrass seeds starch contributed to the reduced extraction yield, particularly when using the aqueous method, as compared to other raw materials.

3.7 | XRD

The XRD obtained indicates that the AE (Figure 1C1) and RE starches (Figure 1C2) exhibit similarities in the intensities of their most prominent peaks, as well as in the intensity and shape of the background. The starches extracted from ryegrass seeds (AE and RE starch) exhibited characteristic properties of type A starch, resembling those of cereal starches, with indications of type V crystallinity behavior (Figure 1C1,C2). The degree of crystallinity (X_c) was determined based on the ratio of the areas under the "Rietveld Refinement" curve (depicted in red) and the 13-term Chebyshev polynomial (depicted in green) (Figure 1C1,C2). The contribution of the sample holder peaks was excluded during the

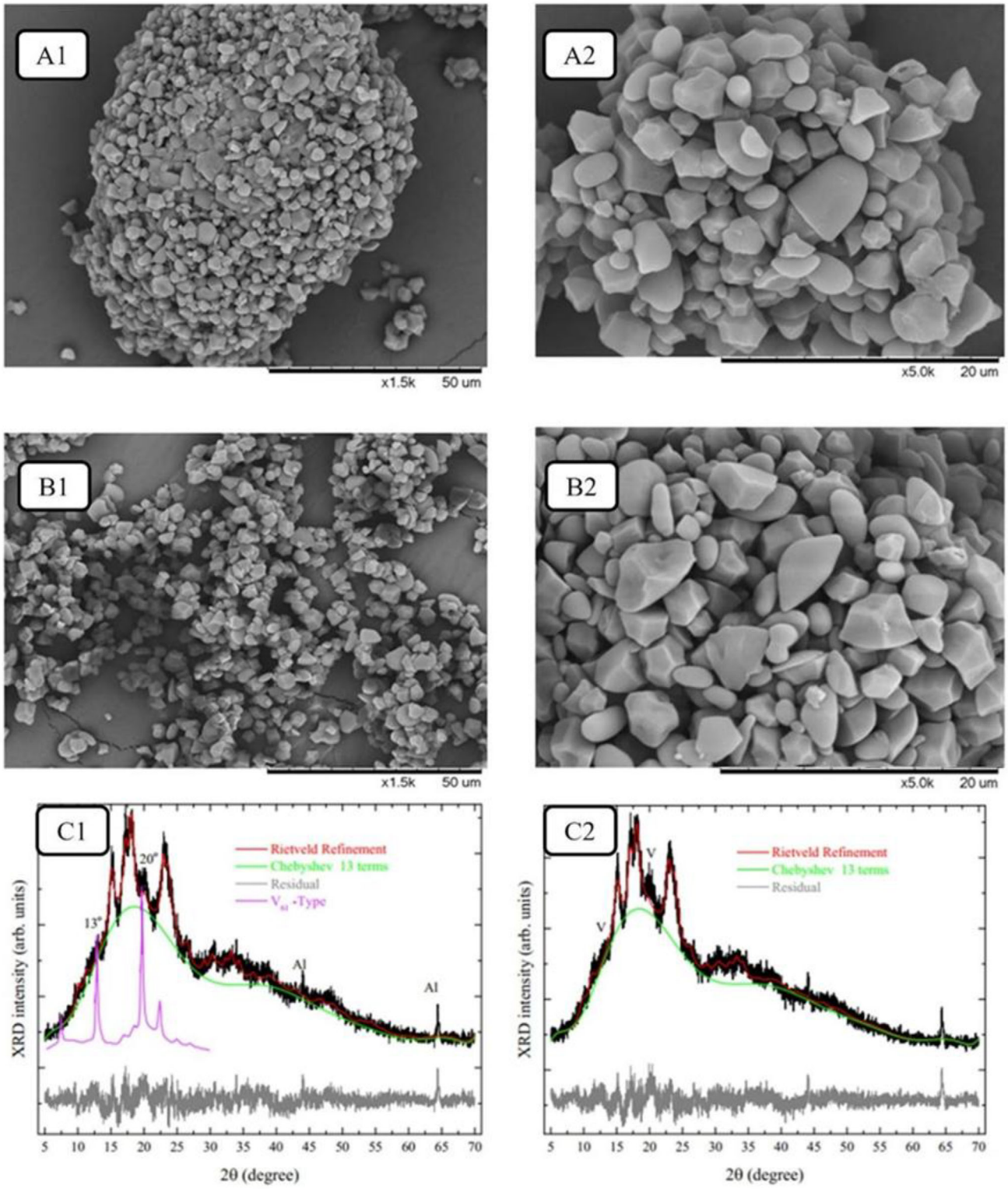

FIGURE 1 | Micrographs from aqueous (A1 = 1500×; A2 = 5000×) and reduction extraction (B1 = 1500×; B2 = 5000×) and x-ray diffractograms of aqueous (C1) and reduction extraction (C2) of ryegrass starches.

calculation. The crystallinity values and the corresponding unit cell parameters are provided in Table S2.

The crystallinity analysis revealed that AE starch exhibited the highest crystallinity value (approximately 13.90%), whereas RE starch displayed a slightly lower value (12.20%). These findings align with the observed apparent amylose content, as RE starch (17.25%) contained significantly more amylose than AE starch (16.90%). This outcome was expected, as amylopectin is the primary contributor to the semi-crystalline organization of starch granules. Ryegrass seed starch exhibited a crystallinity pattern like that of cereal starches, which predominantly display A-type

crystallinity. This pattern is characterized by intensity peaks at approximately 15.3°, 17.1°, 18.2°, and 23.5° [27].

A fourth crystalline type, type V, was identified in the present study. This polymorph results from the crystallization of amylose with lipids and is associated with diffraction intensity peaks at 2θ angles of approximately 12.6°, 13.2°, 19.4°, and 20.6°. The most prominent peaks of the type V polymorph corresponded to 2θ values near 13° and 20°. The precise mechanism underlying the formation of amylose–lipid complexes remains uncertain. One proposed hypothesis posits that, in the presence of a monoacyl lipid, the amylose helix forms and encapsulates the lipid within its cavity. An alternative proposition suggests that the double helix structure of amylose exists inherently, with the monoacyl lipid later integrating into the central cavity [28].

3.8 | FTIR

The typical FTIR spectra of ryegrass seeds AE and RE starches are presented in Figure 2A. In the range of 800 to 1200 cm^{-1} (Figure 2B), the vibration band of the glucan ring is overlapped by the COH stretching and bending vibration bands, as well as the C-O-C glycosidic bond vibration. The band at 1080 cm^{-1} corresponds to C-O bond stretching, while the band at 1105 cm^{-1} indicates the C-C bond stretching. The band at 1022 cm^{-1} is characteristic of a type A crystallinity pattern in starch. The band at 982 cm^{-1} is attributed to CO stretching vibrations. Additionally, a peak observed at 1535 cm^{-1} is associated with strongly bound water, which is attributed to the hygroscopic nature of starch [29].

Starch granules generally contain two distinct water populations: one integrated into the hydrogen bonding network of the starch crystal structure, and the other existing as hydration water, which is less strongly bound. Hydration water appears in the spectra as a broad band between 3000 and 3800 cm^{-1}. The band at 945 cm^{-1} is attributed to C-O-C vibrations within the α-1,4 glycosidic bonds of the starch structure, whereas the band at 860 cm^{-1} is associated with C-H bonds in the CH_2 deformation mode [30].

The peak at 790 cm^{-1} corresponds to the vibration of the -CH_3 group, which may be linked to amino acid residues and lipid presence, as starch itself does not inherently possess a -CH_3 group. This observation supports the presence of the type V crystallinity profile previously discussed, suggesting that the amylose–lipid complex may have formed during the extraction process. The band at 720 cm^{-1} reflects the vibrational properties characteristic of Si-O-Si bonds in silanol-related structures [31]. This finding is consistent with the ash content analysis, as AE and RE starches exhibited a high silicon content, exceeding 20% of the total ash content.

3.9 | DSC

Figure 2C shows the thermogram obtained for one of the replicates evaluated of the ryegrass seeds AE and RE starches, through which we can observe quite similar average values between the ryegrass seeds starches, being T_{on} = 58.13°C, T_{peak} = 64.73°C, and T_{end} = 72.36°C, for the AE starch, and T_{on} = 58.12°C, T_{peak} = 64.51°C, and T_{end} = 74.19°C, for the RE starch. The depression observed in the thermogram corresponds to the endothermic gelatinization transition, which reflects the disruption of the ordered regions within starch granules and is quantified as the gelatinization enthalpy (ΔH). The ΔH values obtained for the starches extracted by AE and RE were 9.08 and 6.14 $J{\cdot}g^{-1}$, respectively, with a statistically significant difference between them ($p < 0.001$). The ΔH can be correlated to the crystallinity of amylopectin and the strength with which the double helices formed by its chains are associated in the granule. Thus, the higher the ΔH, the greater the force required to break the granule structure, which results in gelatinization [32].

3.10 | Physicochemical and Pasting/Gel Properties

3.10.1 | Swelling Power and Solubility

Figure 3A illustrates that the swelling power increased approximately 2.24 fold for AE starch and 2.32 fold for RE starch. Notably, at a temperature of 80°C, the swelling power of the RE sample exceeded that of AE (p = 0.041). No significant differences in solubility (Figure 3B) were observed between the samples as the temperature increased, with solubility increasing by 2.10 fold for AE and 2.57 fold for RE. Statistical analyses were conducted separately for each temperature across all samples.

It was also observed that the starches exhibited high swelling power at elevated temperatures. This behavior is likely attributed to the high amylopectin content and crystalline structure of the starch, as indicated by prior analyses. Additionally, the small size of the starch granules appears to contribute to this phenomenon by requiring greater thermal energy to induce granule swelling.

3.10.2 | Pasting Properties

The pasting properties of ryegrass seed starch are presented in Table 2. It was observed that AE and RE starches did not exhibit a significant difference in the thermal energy required for the onset of granule swelling. However, the pasting temperatures (94.6°C and 95.0°C, respectively) were relatively high compared to those of commercial starches with similar amylose content. Examples include native starches from maize (71.86°C) and sorghum (71.70°C) [33, 34]. This higher pasting temperature is likely attributable to the structural organization of the granules. In addition to their small size, the amylose and amylopectin chains are tightly packed, unlike the looser arrangement observed in potato starch [35].

According to Carvalho et al. [5], the high pasting temperature may be related to strong intramolecular interactions among starch components, primarily driven by the highly branched structure of amylopectin. In contrast, the difference between the temperatures observed by DSC and viscoamylography is due to the distinct principles of each technique. DSC detects the onset of gelatinization, which refers to the initial structural changes in the crystalline regions of starch granules, occurring at lower

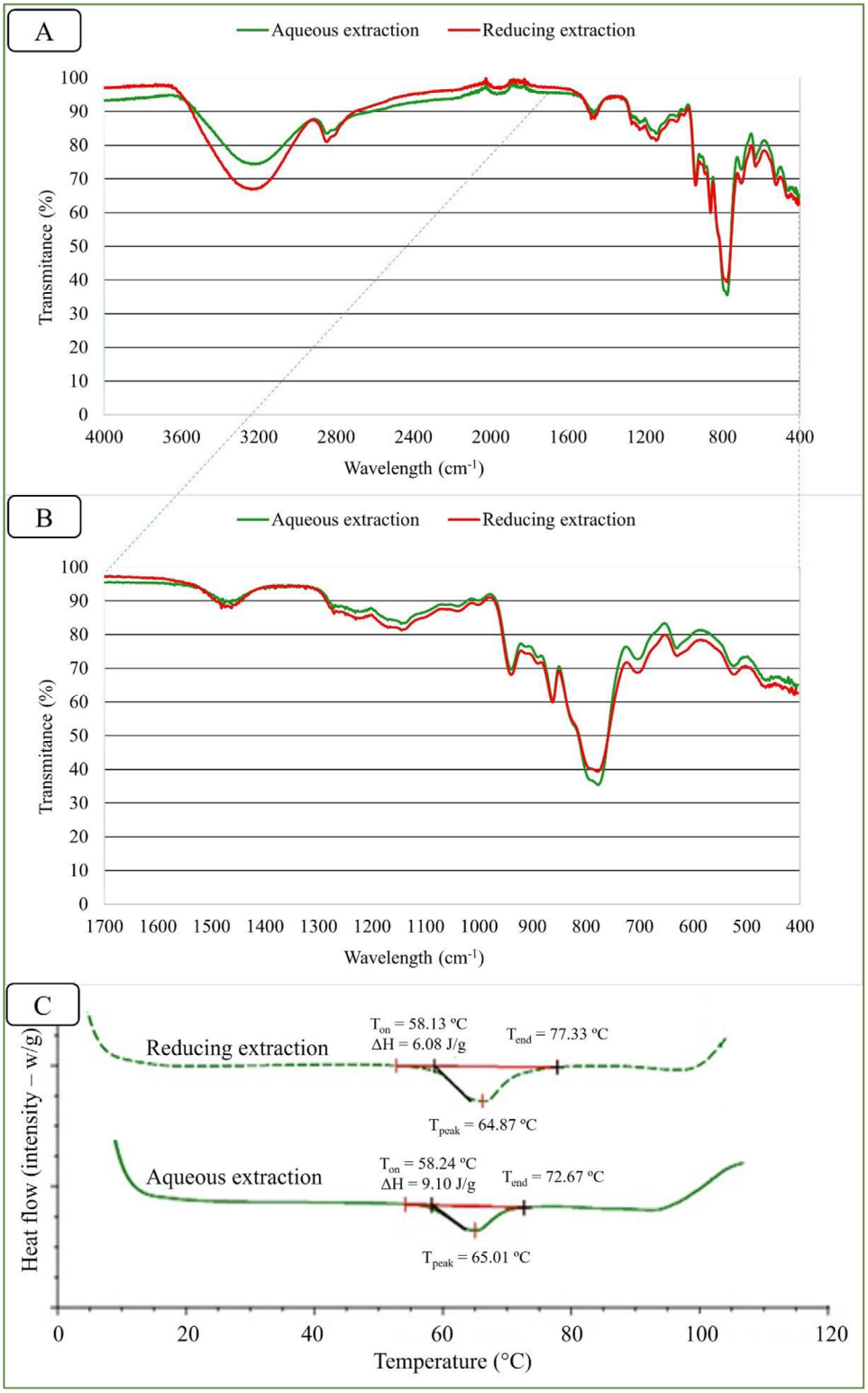

FIGURE 2 | Infrared spectra (A, B) and thermograms (C) of ryegrass starches obtained by aqueous and reducing extractions.

temperatures. Viscoamylography, on the other hand, measures viscosity resulting from the full swelling and rupture of granules, processes that occur at more advanced stages and therefore at higher temperatures. This difference exists because DSC is more sensitive to early molecular transitions, while viscoamylography requires more intense physical changes, such as a significant increase in viscosity [36, 37].

Regarding viscosity, both starches exhibited values above the expected range, as smaller granules typically result in lower viscosities [38]. For the ryegrass seeds starch, AE starch (3637.7 cP) demonstrated a significantly higher peak viscosity compared to RE starch (3205 cP). It has been suggested by Schmiele et al. [12] that starches with higher peak viscosities tend to have a greater proportion of long amylopectin chains, with

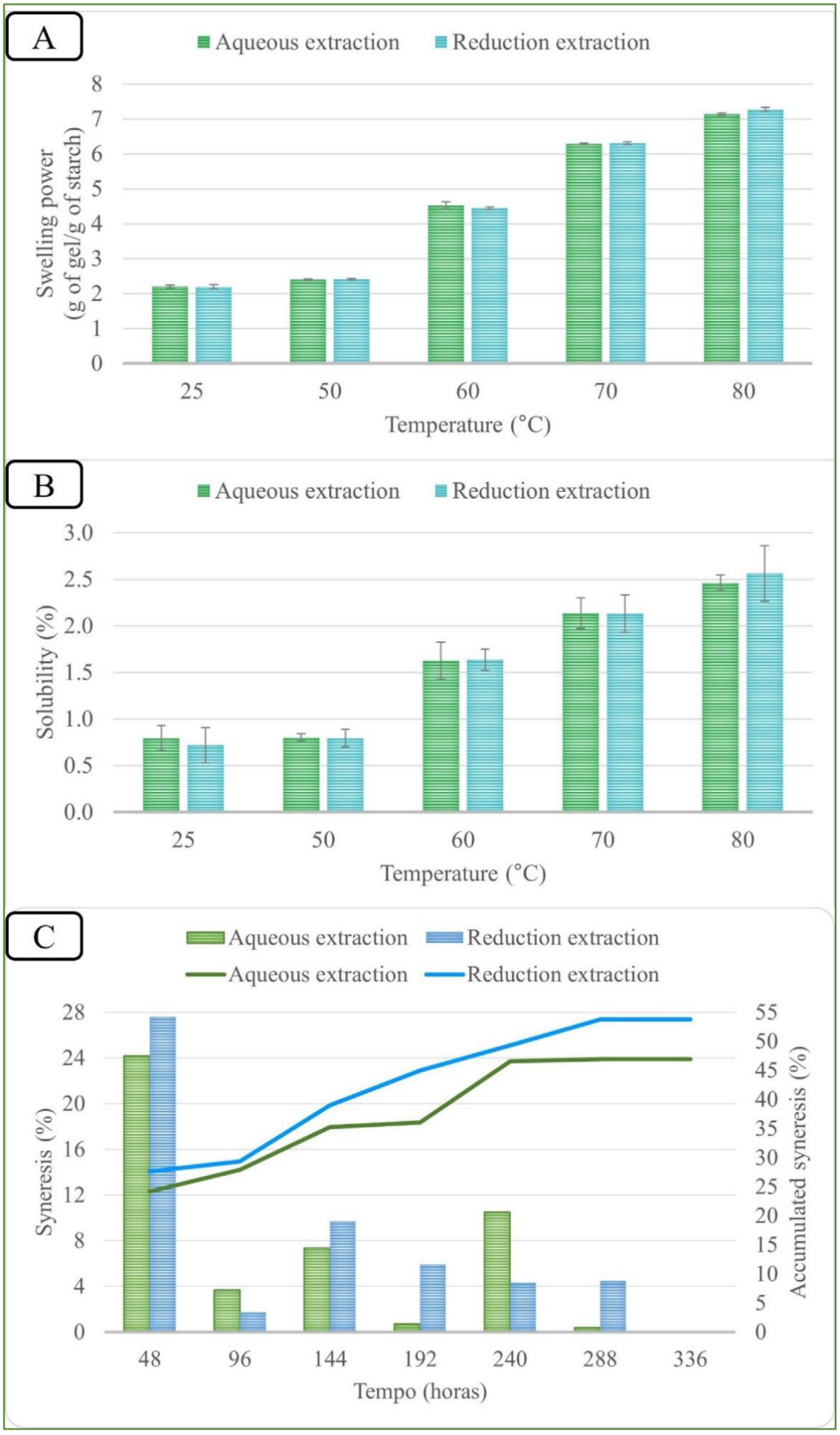

FIGURE 3 | Swelling power (A), solubility (B), and freeze-thaw syneresis (C) of ryegrass starches obtained by aqueous and reducing extractions.

TABLE 2 | Pasting properties of ryegrass starches obtained by aqueous and reducing extractions.

Parameters	Aqueous extraction starch	Reducing extraction starch	*p* value
Peak viscosity (mPa.s)	3638 ± 33	3205 ± 9	< 0.001
Breakdown (mPa.s)	1289 ± 180	807 ± 47	0.021
Relative breakdown (%)	35.41	25.19	0.042
Final viscosity (mPa.s)	4841 ± 47	5352 ± 182	0.004
Setback (mPa.s)	2492 ± 114	2954 ± 122	0.018
Relative setback (%)	51.50	55.18	0.163
Peak time (min)	6.67 ± 0.05	6.50 ± 0.08	0.014
Pasting temperature (°C)	94.60 ± 0.12	95.00 ± 0.39	0.184

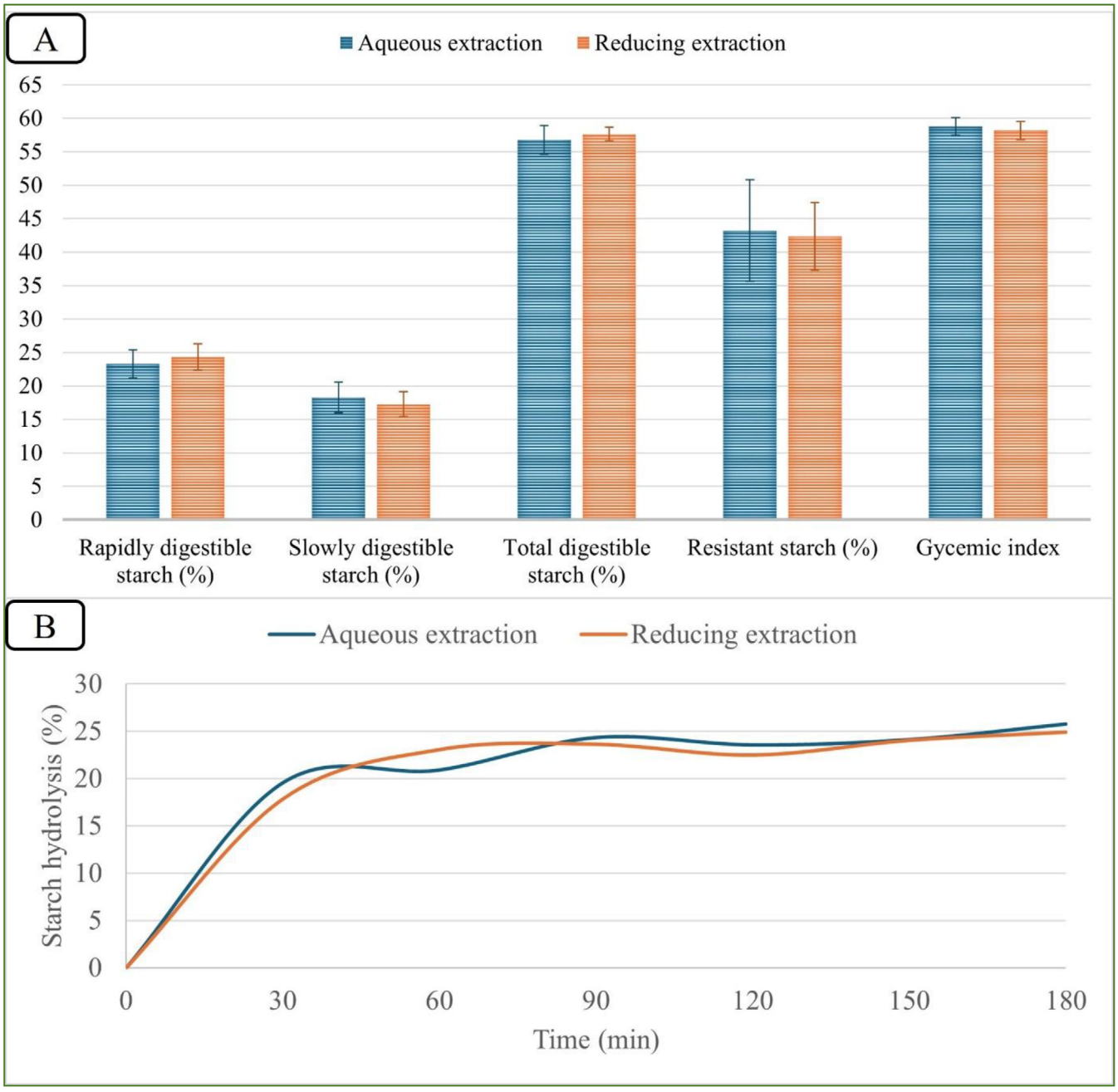

FIGURE 4 | Digestibility, glycemic index (A), and hydrolysis behavior (B) of ryegrass starches obtained by aqueous and reducing extractions.

a maximum degree of polymerization between 70 and 80. In terms of retrogradation tendency, RE starch (2954 cP) displayed higher values than AE starch (2492.3 cP), indicating a lower recrystallization of its amylose molecules [27], with potential use for biodegradable films. In starch-based biodegradable films, high viscosity and high retrogradation rate are closely related properties that significantly influence film performance. High viscosity reflects strong granule swelling and polymer entanglement, which contribute to a cohesive, uniform gel matrix, essential for forming durable, flexible films with good barrier properties. Meanwhile, a high retrogradation rate, particularly from amylose reassociation, enhances the structural integrity and tensile strength of the film by forming crystalline zones within it. Together, these properties reinforce the film during and after drying; however, excessive retrogradation can reduce flexibility and lead to brittleness. Therefore, an optimal balance of high viscosity and controlled retrogradation is key to achieving films that are both strong and functional for biodegradable applications [39]. Concerning peak time, AE starch exhibited a greater value than RE starch, which supports the swelling property of starch, as starches with lower peak times demonstrate greater swelling capacities.

Overall, RE starch exhibited variations in several properties when compared to AE starch, including a higher damaged starch content, reduced crystalline area, and consequently lower viscosity and peak time, along with an increased tendency toward retrogradation. These differences are likely attributable to the effect of SO_2 on the rheological characteristics of RE starch. Starch granules are rendered insoluble in cold water due to the presence of hydrogen bonds and the high crystallinity of their molecular structure. When dispersed in water and heated below their glass transition temperature (T_g), the granules undergo swelling, resulting in a significant increase in size. During this process, the molecular structure of starch is disrupted, leading to the leaching of amylose. The leached amylose forms a three-dimensional network, which contributes to the observed increase in paste viscosity. The starch paste produced comprises a heterogeneous mixture of components, including unswollen granules, partially swollen granules, aggregates of swollen granules, granule fragments, retrograded starch molecules, and starch that has either dissolved or precipitated [38].

3.10.3 | Gel Strength

The low values recorded for AE and RE ryegrass seeds starches (0.22 ± 0.01 and 0.23± 0.02 N, respectively; $p = 0.328$) can be attributed to their low amylose content (< 20%). This behavior can be attributed to the higher affinity of amylopectin molecules for water and their ability to form more viscous gels with reduced syneresis. Consequently, systems with higher amylose content require greater mechanical force for gel disintegration. Historically, starchy foods have typically been processed or cooked in excess water prior to human consumption. Under these conditions, the multi-scale ordered structures of starch undergo irreversible disruption through a phase transition known as gelatinization. This phenomenon is characterized by short-term amylose gelation and long-term amylopectin recrystallization. The gel strength and water mobility in retrograded starch are significantly influenced by the quantity of residual short-range molecular structures that remain following gelatinization [40].

3.10.4 | Paste Clarity

The paste clarity for RE starch (17.71 ± 0.20 %) exhibited a significantly ($p < 0.001$) higher transmittance value compared to the AE starch (8.85 ± 0.02%). This finding aligns with the results observed for the L^* color parameter and visual observations (Table S1). The greater paste clarity of the RE starch may be attributed to the degradation of phenolic compounds by the reducing component and the enzymatic inhibition potentially promoted by it, resulting in a lighter appearance of the RE starch. Additionally, this difference could be explained by the proximate composition (Table 1), as the RE starch contains lower lipid and protein contents, which contribute to its lighter appearance due to increased purity.

3.10.5 | Freeze-Thaw Syneresis

The syneresis graph spans from 48 to 336 h (Figure 3C), demonstrating that water loss decreased to values close to zero in both samples over the cycles. The highest SP for AE and RE starches was observed at 48 h, reaching 24.20% and 27.58%, respectively. Overall, the curves indicate that AE starch exhibited lower water loss, resulting in a more stable gel. These findings align with the paste properties (Table 2), where AE starch displayed a reduced tendency toward retrogradation [27]. The behavior of accumulated syneresis can be represented through nonlinear regression, as shown in Equations (7) and (8). Upon analyzing the angular coefficients of the equations, it is evident that the RE system exhibited a higher value. This model demonstrated a superior fit to the results, as indicated by the highest regression coefficient. Conversely, the AE system displayed a lower regression coefficient, suggesting greater variability in the syneresis values.

$$\text{Aqueousextraction(AE)} = 13.169\ln(x) + 21.648; r = 0.912 \quad (7)$$

$$\text{Reducingextraction(RE)} = 15.355\ln(x) + 23.827; r = 0.9302 \quad (8)$$

3.11 | Starch Digestibility and GI

The results presented in Figure 4A indicate that the extraction method involving a reducing agent resulted in a slight increase in the fraction of TDS ($p < 0.001$) and RDS ($p = 0.037$), while other fractions, such as RS and SDS, remained unaffected. However, these changes have minimal impact on the integrity of the granules concerning starch hydrolysis (Figure 4B), as the GI remains unaffected (Figure 4A), thus corroborating the results observed for damaged starch.

The effect observed in the TDS fraction may be attributed to chemical modifications induced by the reducing agent, such as the alteration of disulfide bonds or the breakdown of aggregates, which make the starch more accessible to digestion. However, the practical implications of these modifications should be evaluated

in broader contexts, such as in situ and in vivo studies, including food formulations, specific health regimes, or interactions with other dietary components [41].

These findings provide valuable insights into the nutritional properties of ryegrass seed starch, particularly given its high content of RS (> 42%). Carvalho et al. [23] explain that RS represents a fraction of starch that is not digested in the small intestine and thus reaches the colon, where it may be fermented by microorganisms, promoting prebiotic effects. The elevated levels of this unconventional starch type suggest potential health benefits, including improved glycemic control due to a slower glucose release into the bloodstream, enhanced satiety (supporting weight management), and the production of short-chain fatty acids in the colon, which are associated with gut health and immune function.

As outlined by Capriles et al. [42], when glucose is used as the reference product, the GI can be classified as low (< 55), moderate (56–69), or high (> 70). The GI of ryegrass seeds starch, approximately 58, classifies it as moderate, indicating that it does not elevate glucose levels as rapidly as high-GI foods. The high content of RS contributes to this result, as a significant portion of the starch is not rapidly digested. These characteristics render ryegrass seed starch a promising candidate for food applications aimed at promoting health and well-being, still in its native form, without the need for modification. Although most starches from unconventional sources have significant RS content, with values above 70%, such as mango kernel (73.73%) [43], purple yam (*Dioscorea alata* L.) (81.3%) [44], and ginger (*Rhizoma curcumae* longae) (77.99%) [45], some of them have low values, around 9.3 to 2.1% like cowpea (*Vigna unguiculata* L. Walp.) [46], approximately 15.0% for lotus seed (*Nelumbo nucifera* Gaertn.) [47], and 25.0% for arrowroot (*Calathea allouia*) [48].

4 | Conclusion

Ryegrass seeds have been identified as a promising unconventional raw material, primarily due to their significant starch content, which exhibits desirable characteristics for both food and non-food industries. The starch extracted from ryegrass seeds has demonstrated potential for different applications, since it exhibited properties comparable to those of traditionally used starches, especially in bakery products, as well as in the production of bioplastics, biodegradable films, and formulations for cosmetics, pharmaceuticals, and personal hygiene products, among others. Additionally, this starch offers the additional advantage of not altering the color of the final product.

This study represents a pioneering effort in the characterization of ryegrass seed starch, aiming to add value to a previously undervalued raw material. Ryegrass is notably resistant to pesticides and highly adaptable to a wide range of soil types and climatic conditions. In this way, a seed formerly used only as animal fodder may now assume a more prominent role, enhancing its market value, supporting regional development and local culture, and benefiting small and medium producers. Furthermore, it offers a new source of starch that can be obtained through a more sustainable process.

Nevertheless, further research is necessary to optimize the starch extraction process, assess its in vivo digestibility, and evaluate its potential as a substitute for conventional starches, such as corn, cassava, potato, and rice, to substantiate its viability as a novel ingredient for industrial applications.

Author Contributions

Thaís Silveira Pimenta: methodology, software, validation, formal analysis, investigation, writing – original draft preparation, visualization. **Geycson Figueiredo Dias**: methodology, formal analysis, investigation, writing – original draft preparation, visualization. **Hugo José Martins Carvalho**: methodology, formal analysis, software, investigation, writing – original draft preparation, visualization. **Nathalia de Andrade Neves**: methodology, software, validation, investigation, data curation, visualization. **Sérgio Michielon de Souza**: methodology, software, validation, formal analysis, investigation, visualization. **Carlos Wanderlei Piler de Carvalho**: methodology, software, validation, formal analysis, investigation, visualization. **Elizabeth Harumi Nabeshima**: methodology, software, validation, formal analysis, investigation, visualization. **Izabela Dutra Alvim**: methodology, software, formal analysis, visualization. **Maria Teresa Pedrosa Silva Clerici**: conceptualization, methodology, investigation, resources, data curation, writing – review and editing, visualization. **Mária Herminia Ferrari Felisberto**: conceptualization, methodology, software, validation, formal analysis, investigation, resources, data curation, writing – review and editing, visualization, supervision. **Marcio Schmiele**: conceptualization, methodology, software, validation, investigation, resources, data curation, writing – review and editing, visualization, supervision, project administration, funding acquisition. All authors have read and agreed to the published version of the manuscript.

Acknowledgments

The authors thank the National Council for Scientific and Technological Development (CNPq) for the scholarship awarded to G. F. Dias (#134657/2021-7) and research productivity fellowship to M. T. P. S. Clerici (#312660/2023-5) and M. Schmiele (#312759/2025-8), the Coordination for the Improvement of Higher Education Personnel (CAPES) for financial support (funding code 001) and the scholarships of T. S. Pimenta (#88887.601647/2021-00) and H. J. M. Carvalho (#88887.822278/2023-00), and the Minas Gerais Research Foundation (FAPEMIG) for financial support (#APQ-01456-21).

Conflicts of Interest

The authors declare no conflicts of interest.

Data Availability Statement

Data will be made available on request.

References

1. C. C. Fernandes Filho, M. H. M. L. Andrade, J. A. R. Nunes, et al., "Breeding for Drought Tolerance in Perennial Ryegrass (*Lolium perenne* L.) and Tall Fescue (*Lolium arundinaceum* [Schreb.] Darbysh.) by Exploring Genotype by Environment by Management Interactions," *Grassland Research* 2, no. 1 (2023): 22–36, https://doi.org/10.1002/glr2.12045.

2. C. T. Lima, T. M. Santos, N. A. Neves, et al., "New Breakfast Cereal Developed With Sprouted Whole Ryegrass Flour: Evaluation of Technological and Nutritional Parameters," *Foods* 12, no. 21 (2023): 3902, https://doi.org/10.3390/foods12213902.

3. R. M. Dereti, *Boas Práticas Agropecuárias na Produção de Leite: Da Pesquisa para o Produtor* (Embrapa Clima Temperado, 2017), http://www.infoteca.cnptia.embrapa.br/infoteca/handle/doc/1078090.

4. Q. Feng, S. Song, Y. Yang, M. Amee, L. Chen, and Y. Xie, "Comparative Physiological and Metabolic Analyzes of Two Italian Ryegrass (*Lolium multiflorum*) Cultivars With Contrasting Salinity Tolerance," *Physiologia Plantarum* 172, no. 3 (2021): 1688–1699, https://doi.org/10.1111/ppl.13374.

5. H. J. M. Carvalho, L. H. R. Oliveira, G. J. S. Souza, et al., "Unraveling Sudan Grass Starch: A First Report of Its Physicochemical, Structural, Technological, and Nutritional Properties," *Food and Humanity* 4 (2025): 100627, https://doi.org/10.1016/j.foohum.2025.100627.

6. S. Pérez-Vila, M. Fenelon, D. Hennessy, J. A. O'Mahony, and L. G. Gómez-Mascaraque, "Impact of the Extraction Method on the Composition and Solubility of Leaf Protein Concentrates From Perennial Ryegrass (*Lolium perenne* L.)," *Food Hydrocolloids* 147 (2024): 109–372, https://doi.org/10.1016/j.foodhyd.2023.109372.

7. J. D. Wilson, D. B. Bechtel, T. C. Todd, and P. A. Seib, "Measurement of Wheat Starch Granule Size Distribution Using Image Analysis and Laser Diffraction Technology," *Cereal Chemistry* 83 (2006): 259–268, https://doi.org/10.1094/CC-83-0259.

8. K. J. Goering, "Some Anomalies in Starch Chemistry Are They due to Granule Structure?" *Starch-Stärke* 30, no. 6 (1978): 181–183, https://doi.org/10.1002/star.19780300602.

9. B. L. Tagliapietra, B. G. Melo, E. A. Sanches, M. Plata-Oviedo, P. H. Campelo, and M. T. P. S. Clerici, "From Micro to Nanoscale: A Critical Review on the Concept, Production, Characterization, and Application of Starch Nanostructure," *Starch-Stärke* 73, no. 11–12 (2021): 2100079, https://doi.org/10.1002/star.202100079.

10. AACCI (American Association of Cereal Chemists International), *Approved Methods*, 11th ed. (AACC International, 2010).

11. S. L. M. El Halal, D. H. Kringel, E. R. Zavareze, and A. R. G. Dias, "Methods for Extracting Cereal Starches From Different Sources: A Review," *Starch-Stärke* 71, no. 11–12 (2019): 1900128, https://doi.org/10.1002/star.201900128.

12. M. Schmiele, G. A. R. Sehn, V. S. Santos, et al., "Physicochemical, Structural and Rheological Properties of Chestnut (*Castanea sativa*) Starch," *American Journal of Food Science and Technology* 3, no. 4A (2015): 1–7, https://doi.org/10.12691/ajfst-3-4A-1.

13. A. L. Fadini, I. D. Alvim, K. B. F. Paganotti, et al., "Optimization of the Production of Double-Shell Microparticles Containing Fish Oil," *Food Science and Technology International* 25 (2019): 359–369, https://doi.org/10.1177/1082013219825890.

14. H. S. Jang, J. Lee, H. J. Lee, and E. Y. Park, "Phytate-mediated Phosphorylation of Maize, Rice, and Potato Starches at Different pH Conditions," *International Journal of Biological Macromolecules* 165 (2020): 857–864, https://doi.org/10.1016/j.ijbiomac.2020.09.245.

15. Y. Wu, M. Niu, and H. Xu, "Pasting Behaviors, Gel Rheological Properties, and Freeze-Thaw Stability of Rice Flour and Starch Modified by Green Tea Polyphenols," *LWT—Food Science Technology* 118 (2020): 108796, https://doi.org/10.1016/j.lwt.2019.108796.

16. I. Goñi, A. Garcia-Alonso, and F. Saura-Calixto, "A Starch Hydrolysis Procedure to Estimate Glycemic Index," *Nutrition Research* 17, no. 3 (1997): 427–437, https://doi.org/10.1016/S0271-5317(97)00010-9.

17. B. A. Acosta-Estrada, S. O. Serna-Saldívar, and C. Chuck-Hernández, "Quality Assessment of Maize Tortillas Produced From Landraces and High Yield Hybrids and Varieties," *Frontiers in Nutrition* 10 (2023): 1105619, https://doi.org/10.3389/fnut.2023.1183935.

18. M. A. Scariot, B. Rohrig, R. S. Barok, R. G. Dionello, and L. L. Radünz, "Kinetic of Drying of Rice Grains at Different Temperatures Using Dry and Damp Firewood as Calorific Energy Supply," *Agricultural Engineering International: CIGR Journal* 23, no. 4 (2021): 219–226.

19. A. Tessema and H. Admassu, "Extraction and Characterization of Starch From Anchote (*Coccinia abyssinica*): Physico-Chemical, Functional, Morphological and Crystalline Properties," *Journal of Food Measurement and Characterization* 15 (2021): 3096–3110, https://doi.org/10.1007/s11694-021-00885-y.

20. L. R. Silva, C. W. P. Carvalho, J. I. Velasco, and F. M. Fakhouri, "Extraction and characterization of Starches From Pigmented Rice," *International Journal of Biological Macromolecules* 156 (2020): 485–493, https://doi.org/10.1016/j.ijbiomac.2020.04.034.

21. J. Liu, X. S. Yu, Y. D. Wang, G. H. Fang, and Y. W. Liu, "A Cleaner Approach for Corn Starch Production by Ultrasound-Assisted Laboratory Scale Wet-Milling," *Food Science and Technology Research* 26, no. 4 (2020): 469–478, https://doi.org/10.9721/KJFST.2021.53.6.731.

22. B. P. Costa, D. Carpiné, F. E. S. B. Alves, et al., "Thermal, Structural, Morphological and Bioactive Characterization of Acid and Neutral Modified Loquat (*Eriobotrya japonica* Lindl.) Seed Starch and Its By-products," *Journal of Thermal Analysis and Calorimetry* 147 (2022): 6721–6737, https://doi.org/10.1007/s10973-021-10965-2.

23. H. J. M. Carvalho, M. T. Barcia, and M. Schmiele, "Non-Conventional Starches: Properties and Potential Applications in Food and Non-Food Products," *Macromolecular Symposia* 4, no. 4 (2024): 886–909, https://doi.org/10.3390/macromol4040052.

24. T. A. Medeiros, V. Y. Suzuki, J. A. T. M. Leite, et al., "Silício nos Alimentos: Uma Revisão," *Advances in Nutritional Sciences* 1, no. 1 (2020): 41–48, https://doi.org/10.47693/ans.v1i1.7.

25. A. K. Rashwan, H. A. Younis, A. M. Abdelshafy, et al., "Plant Starch Extraction, Modification, and Green Applications: A Review," *Environmental Chemistry Letters* 22 (2024): 2483–2530, https://doi.org/10.1007/s10311-024-01753-z.

26. F. Zhu, "Impact of Ultrasound on Structure, Physicochemical Properties, Modifications, and Applications of Starch," *Trends in Food Science & Technology* 43, no. 1 (2015): 1–17, https://doi.org/10.1016/j.tifs.2014.12.008.

27. H. J. M. Carvalho, S. M. Souza, C. W. P. Carvalho, E. H. Nabeshima, and M. Schmiele, "Cocoyam Is an Unconventional, Innovative, and Sustainable Source of Starch With Potential Use in Sleek and Functional Biodegradable Films," *Starch-Stärke* 77, no. 3 (2024): 2400125, https://doi.org/10.1002/star.202400125.

28. X. Zhao, T. Mei, and B. Cui, "Lipids-Modified Starch: Advances in Structural Characteristic, Physicochemical Property, and Application," *Food Research International* 197 (2024): 115146, https://doi.org/10.1016/j.foodres.2024.115146.

29. A. M. Nzenguet, M. Aqlil, Y. Essamlali, et al., "Novel Bionanocomposite Films Based on Graphene Oxide Filled Starch/Polyacrylamide Polymer Blend: Structural, Mechanical and Water Barrier Properties," *Journal of Polymer Research* 25 (2018): 86, https://doi.org/10.1007/s10965-018-1469-7.

30. R. Sindhu and B. S. Khatkar, "Thermal, Structural and Textural Properties of Amaranth and Buckwheat Starches," *Journal of Food Science and Technology* 55 (2018): 5153–5160, https://doi.org/10.1007/s13197-018-3474-6.

31. A. Tohry, R. Dehghan, P. Hatefi, and S. C. Chelgani, "A Comparative Study Between the Adsorption Mechanisms of Sodium Co-Silicate and Conventional Depressants for the Reverse Anionic Hematite Flotation," *Separation Science and Technology* 57, no. 1 (2022): 141–158, https://doi.org/10.1080/01496395.2021.1887893.

32. L. M. Fonseca, S. L. M. El Halal, A. R. G. Dias, and E. R. Zavareze, "Physical Modification of Starch by Heat-Moisture Treatment and Annealing and Their Applications: A Review," *Carbohydrate Polymers* 274, no. 15 (2021): 118665, https://doi.org/10.1016/j.carbpol.2021.118665.

33. E. Morales-Sánchez, M. Gaytán-Martínez, M. E. Rodriguez-García, M. M. BM, and A. H. Cabrera-Ramírez, "Behavior of Pasting Properties of Ohmic-Heated Corn Starch Versus Moisture and Temperature Applied," *Starch-Stärke* 76, no. 5–6 (2024): 2200245, https://doi.org/10.1002/star.202200245.

34. T. Li, J. Huang, J. Yu, X. Tian, C. Zhang, and H. Pu, "Effects of Soaking Glutinous Sorghum Grains on Physicochemical Properties of Starch," *International Journal of Biological Macromolecules* 267 (2024): 131522, https://doi.org/10.1016/j.ijbiomac.2024.131522.

35. D. Ahmad, Y. Ying, and J. Bao, "Understanding Starch Biosynthesis in Potatoes for Metabolic Engineering to Improve Starch Quality: A Detailed

Review," *Carbohydrate Polymers* 346 (2024): 122592, https://doi.org/10.1016/j.carbpol.2024.122592.

36. J. Qian and M. Kuhn, "Evaluation on Gelatinization of Buckwheat Starch: A Comparative Study of Brabender Viscoamylography, Rapid Visco-Analysis, and Differential Scanning Calorimetry," *European Food Research and Technology* 209 (1999): 277–280, https://doi.org/10.1007/s002170050493.

37. E. E. Péret, W. M. Breene, and Y. A. Bahnassey, "Gelatinization Profiles of Peruvian Carrot, Cocoyam and Potato Starches as Measured With the Brabender Viscoamylograph, Rapid Visco-Analyzer, and Differential Scanning Calorimeter," *Starch/Stärke* 50 (1998): 14–16, https://doi.org/10.1002/(SICI)1521-379X(199801)50:1⟨14.

38. K. Shevkani, N. Singh, N. Isono, and T. Noda, "Structural and Functional Properties of Amaranth Starches From Residue Obtained During Protein Extraction," *Journal of Food Measurement and Characterization* 15 (2021): 5087–5096, https://doi.org/10.1007/s11694-021-01070-x.

39. M. Muratkhan, K. Zhainagul, Y. Yermekov, et al., "Comparable Analysis of Natural and Modified Starches From Kazakhstan: Physicochemical Properties, Applications, and Insights on Biodegradable Films," *Applied Sciences* 15, no. 7 (2025): 3938, https://doi.org/10.3390/app15073938.

40. X. Liu, C. Chao, J. Yu, L. Copeland, and S. Wang, "Mechanistic Studies of Starch Retrogradation and Its Effects on Starch Gel Properties," *Food Hydrocolloids* 120 (2021): 106914, https://doi.org/10.1016/j.foodhyd.2021.106914.

41. J. Singh, A. Dartois, and L. Kaur, "Starch Digestibility in Food Matrix: A Review," *Trends in Food Science & Technology* 21, no. 4 (2010): 168–180, https://doi.org/10.1016/j.tifs.2009.12.001.

42. V. D. Capriles, A. C. Guerra-Matias, and J. A. G. Arêas, "*In Vitro* Marker of Glycemic Response of Foods as a Tool to Aid in Diet Prescription and Evaluation" [in Portuguese], *Revista de Nutrição* 22 (2009): 549–557, https://doi.org/10.1590/S1415-52732009000400010.

43. O. Patiño-Rodríguez, E. Agama-Acevedo, G. Ramos-Lopez, and L. A. Bello-Pérez, "Unripe Mango Kernel Starch: Partial Characterization," *Food Hydrocolloids* 101 (2020): 105490, https://doi.org/10.1016/j.foodhyd.2019.105512.

44. T. Li, F. An, H. Teng, Q. Huang, F. Zeng, and H. Song, "Comparison of Structural Features and in Vitro Digestibility of Purple Yam (*Dioscorea alata* L.) Resistant Starches by Autoclaving and Multi-Enzyme Hydrolysis," *Food Science and Biotechnology* 27 (2018): 27–36, https://doi.org/10.1007/s10068-017-0206-z.

45. X. Li, W. Chen, Q. Chang, Y. Zhang, B. Zheng, and H. Zeng, "Structural and Physicochemical Properties of Ginger (*Rhizoma curcumae* Longae) Starch and Resistant Starch: A Comparative Study," *International Journal of Biological Macromolecules* 144 (2020): 67–75, https://doi.org/10.1016/j.ijbiomac.2019.12.047.

46. CLERICI, Maria Teresa Pedrosa Silva and Marcio Schmiele, eds., *Starches for Food Application: Chemical, Technological and Health Properties* (Academic Press, 2018).

47. G. Giuberti, A. Marti, A. Gallo, S. Grassi, and G. Spigno, "Resistant Starch From Isolated White Sorghum Starch: Functional and Physicochemical Properties and Resistant Starch Retention After Cooking. A Comparative Study," *Starch/Stärke* 71 (2019): 1–9, https://doi.org/10.1002/star.201800194.

48. T. J. Gutiérrez, "Characterization and In Vitro Digestibility of Non-conventional Starches From Guinea Arrowroot and *La Armuña* Lentils as Potential Food Sources for Special Diet Regimens," *Starch/Stärke* 70 (2018): 1–13, https://doi.org/10.1002/star.201700124.

Supporting Information

Additional supporting information can be found online in the Supporting Information section.

Supporting File 1: star70155-sup-0001-TableS1.docx.

Supporting File 2: star70155-sup-0002-TableS2.docx.